This is a preprint to the article published in:
Journal of Sound and Vibration, Vol. 330, No. 22, pp. 5292-5308 (2011).
http://dx.doi.org/10.1016/j.jsv.2011.05.029

Please, cite this document as:
T. G. ZIELIŃSKI. "Numerical investigation of active porous composites with enhanced acoustic absorption." *Journal of Sound and Vibration*, Vol. **330**, No. 22, pp. 5292-5308 (2011).
DOI: 10.1016/j.jsv.2011.05.029

Numerical investigation of active porous composites with enhanced acoustic absorption

TOMASZ G. ZIELIŃSKI
Institute of Fundamental Technological Research, Polish Academy of Sciences
ul. Pawinskiego 5B, 02-106 Warsaw, Poland
e-mail: tzielins@ippt.pan.pl

Abstract

The paper presents numerical analysis – involving an advanced multiphysics modeling – of the concept of active porous composite sound absorbers. Such absorbers should be made up of a layer or layers of poroelastic material (porous foams) with embedded elastic inclusions having active (piezoelectric) elements. The purpose of such active composite material is to significantly absorb the energy of acoustic waves in a wide frequency range, particularly, at lower frequencies. At the same time the total thickness of composite should be very moderate. The active parts of composites are used to adapt the absorbing properties of porous layers to different noise conditions by affecting the so-called solid-borne wave – originating mainly from the vibrations of elastic skeleton of porous medium – to counteract the fluid-borne wave – resulting mainly from the vibrations of air in the pores; both waves are strongly coupled, especially, at lower frequencies. In fact, since the traction between the air and the solid frame of porous medium is the main absorption mechanism, the elastic skeleton is actively vibrated in order to adapt and improve the dissipative interaction of the skeleton and air in the pores. Passive and active performance of such absorbers is analysed to test the feasibility of this approach.

Key words: active foams, poroelasticity, piezoelectricity, multiphysics modeling.

Highlights:

- Acoustic absorption of foams with passive and active inclusions is investigated.
- Multiphysics modeling involves the Biot's poroelasticity, piezoelectricity, etc.
- Passive inclusions enhance absorption at some frequencies, but may also decrease it.
- Active composites are always superior to passive, or foams without inclusions.
- Frame is actively vibrated to enhance dissipative interaction with air in the pores.

1. Introduction

There are apparent reasons for advanced modeling of porous composites of various types, for example, porous media with distributed masses and solid inclusions, which should be at the same time sufficiently accurate and efficient to allow a reliable optimization of such poroelastic composites. Recent experimental investigations report a significant improvement of the insertion loss of standard acoustic blankets at lower frequencies by the addition of randomly placed masses to the poroelastic layers [1]. They show that the improvement by distributed masses (inclusions) tend to be greater than the one due to the mass effect alone. The acoustic absorption of multi-layer absorbers with different inner structures has also become a subject of research [2]. The proposed modeling is accurate with respect to the geometry thanks to the finite-element approach, however, the porous medium is modeled by using the so-called fluid-equivalent approach which generally assumes that the frame (i.e., solid skeleton) of a porous medium is rigid. For many porous materials such approach gives good predictions at higher frequencies and for certain configurations. This is insufficient, however, at lower frequencies and for active systems systems. Another numerical investigation of the problem of an elastic plate with a bonded porous layer involved advanced modeling proposed by Dauchez *et al.* [3]. The modeling applied the theory of poroelasticity for porous medium, yet the problem was purely passive. A recent, pioneering work by Yamamoto *et al.* [4] proposes a new topology optimization method that allows to use poroelastic materials for minimizing the sound pressure levels in a coupled structural-acoustic system. It presents three examples of topology optimization of a 30 mm-thick design domain of passive layers consisting of one or two poroelastic media, elastic inclusions and air cavities.

Research on active-passive broadband noise reducing systems involving porous media started at the very end of 20th century with the publications of papers by Gentry, Guigou, and Fuller [5, 6, 7] on smart foams, that is, polyurethane acoustic foams with sections of PVDF film embedded inside. Such devices are supposed to reduce sound by the simultaneous action of the passive absorption of the foams (effective at high frequencies) and the active input of the PVDF elements driven by an oscillating electrical input (effective at low frequencies). Only experimental investigations were effectuated and the approach was focused mainly on the application of some control algorithms. Recently, a very similar approach was also investigated experimentally for passive-active underwater sound reduction [8]. Similarly, only experimental tests were performed by Lee *et al.* [9] to check feasibility of the concept of the so-called active and passive hybrid panels, that is, panels made up of a layer of porous noise-absorbing material with an aluminum faceplate, or two faceplates and an air gap in case of the so-called double panel. To the aluminum faceplate a piezoelectric patch was fixed. It served as a sensor and actuator for the active approach adopted in the low frequency range, for which (instead of using a complicated controller) a simple negative feedback control was used; and in the passive case the circuit was simply shunt.

Hybrid acoustic treatment combining a porous material and active control techniques was also investigated by Sellen *et al.* [10]. This investigation was carried out for a specific laboratory flow duct and it involved experimental tests as well as some modeling. One aim of modeling was a selection of a passive porous layer and to this end, the rigid-frame, fluid-equivalent model of Allard [11, 12] was applied. Recent works by Galland and Dupont [13, 14] investigate the potential of active absorbers which involve an active control system to cancel the acoustic pressure at the rear face of a porous layer, so as to obtain a purely real impedance at the front face, the value of which depends only on the resistivity and thickness of the porous material.

An advanced fully-coupled approach to model a problem of noise transmission through hybrid acoustic panels has been applied by Galland and her collaborators [15, 16, 17]. By means of advanced modeling techniques they have started to study active-passive sandwich panels with a core of poroelastic material and piezoelectric patches glued to elastic faceplates. The piezoelectric elements as well as the poroelastic core are modeled using fully-coupled theories. Moreover, results presented in papers [15, 16] are purely numerical, while the papers by Batifol *et al.* [18, 17] bring a comparison of results obtained using FE modeling with some analytical developments, showing also some findings of a preliminary experimental test.

Recently, the active-passive concept of smart foams combining the passive dissipation capability of porous material in the medium and high frequency ranges and the active absorption ability of piezoelectric actuator (PVDF) in the low frequency range has been investigated extensively by Leroy *et al.* [19, 20, 21]. To this end, an advanced finite element modeling was performed (involving poroelastic finite elements) with some experimental validation test to demonstrate the validity of the FE model in passive state.

So far, only experimental investigations have been carried out for acoustical properties of the so-called magnetorheological foams, which are highly porous sound absorbing materials with skeleton coated with magnetorheological fluid, in order to test the feasibility of active or adaptive improvement of some desirable properties (like, for example, the acoustic absorption) by the application of magnetic field [22, 23, 24]. The experiments show some potential of this concept and it is obvious that for further investigations some advanced multiphysics modeling would be very helpful.

In the present paper the acoustic absorption of porous composites with active inclusions is examined. The absorption should be actively improved by affecting the vibrations of the elastic skeleton of porous layers. Thus, it is apparent that the rigid-frame approach cannot be used here. Instead, the advanced biphasic theory of poroelasticity is used to model porous material of such active absorbers. This model is substantially different and much more complicated than the commonly used fluid-equivalent approach. Moreover, it will be fully-coupled with the models of elasticity and piezoelectricity needed for passive and active inner structures. Preliminary investigations of this concept were presented in [25].

It is important to observe now that the active approach, which will be discussed here, consists in active improvement of some dissipative mechanism of porous medium, and thus, concerns rather medium and lower frequencies but not very low frequencies. Moreover, since – as it will be shown – the absorption enhancement is not achieved by the generation of attenuating counter-

waves in the air, but rather by an improvement of dissipative mechanism of viscous traction forces between the solid skeleton of porous medium and the air filling the pores, it is expected that this approach should require relatively small voltage signals. It will be shown that the purpose of active inclusions is to create a skeleton movement in the direction of incident waves impinging porous layers, and the fluid in the pores is supposed to be affected mainly by the interaction with the skeleton. In that way it is substantially different from previous approaches proposed for smart foams and hybrid panels. For example, in the work of Leroy *et al.* [21] the porous foam is backed by a PVDF film of curved shape so that the active radial displacements of the film affect – at the same time and in a similar manner – the skeleton *and* the fluid, whereas in the approach examined here the skeleton is actively (dynamically) stretched and the idea is to affect the fluid rather indirectly.

The next section of this paper provide theoretical considerations and background concerning fully coupled multiphysics modeling of the considered problem. The summation convention is used for (dummy) indices $i, j, k, l = 1, 2, 3$, and the (invariant) differentiation symbol which, in the Cartesian coordinate system, simply reads: $(.)_{|i} = \frac{\partial(.)}{\partial x_i}$. Then, in the following sections, a few generic designs of porous composites are presented and the results of the analyses of passive and active performance of these absorbers are discussed.

2. Important modeling issues

2.1. Multiphysics character of modeling

The examined application of active porous composites links several mathematical models, namely: the Biot's theory of poroelasticity – to model the material of porous layer (with air-filled pores); the linear elasticity – to model elastic inclusions; the piezoelectricity – to model the active parts (piezo-actuators) of inclusions which affect the lower-frequency vibrations of the elastic skeleton of a porous medium; the linear acoustics – to model layers or gaps of inviscid, elastic fluids.

The considered vibroacoustic application allows for using linear theories, so the superposition principle holds and may be effectively used. Consequently, the frequency analysis may be used as an efficient tool for design and testing of the proposed active porous composites. Thus, all considered problems are time-harmonic with the frequency f and the angular frequency $\omega = 2\pi f$. Furthermore, the equations of poroelasticity presented below assume no body forces acting on the poroelastic material. Consequently, the problems of elasticity and piezoelectricity are considered with zero body forces. Moreover, in the piezoelectricity problem there is no body electric charge applied. These assumptions comply with the modeling requirements of the active porous composite noise absorbers.

All the involved problems are strongly coupled and the consideration of this mutual interaction of different media is very important. Thus, a coupled multiphysics model of a system made up of poroelastic, elastic, piezoelectric, and acoustic media was constructed [26] using the Galerkin finite-element method and the following weak integral:

$$\mathcal{WF} = \mathcal{WF}_{\mathrm{p}} + \mathcal{WF}_{\mathrm{e}} + \mathcal{WF}_{\mathrm{pz}} + \mathcal{WF}_{\mathrm{a}} + \mathcal{CI}\,, \tag{1}$$

where $\mathcal{WF}_{\mathrm{p}}$, $\mathcal{WF}_{\mathrm{e}}$, $\mathcal{WF}_{\mathrm{pz}}$, $\mathcal{WF}_{\mathrm{a}}$ are the weak forms of poroelasticity, elasticity, piezoelectricity, and acoustics, respectively, whereas $\mathcal{CI}$ is the coupling integral on the interfaces between various media; the weak forms are given in [26]. Some, at least partial – since no porous media were involved – experimental validation of the proposed system was presented in [27].

Basic facts about the Biot's theory of poroelasticity will be briefly recalled below, in Section 2.2. One of these facts is that the harmonic poroelasticity problem can be described by the so-called mixed formulation which uses as dependent variables the solid phase displacements, u_i, and the pore-fluid pressure, p. The corresponding weak form $\mathcal{WF}_{\mathrm{p}}$ is given in [28, 12, 26] where the boundary conditions are also discussed; an exhaustive discussion of boundary conditions can be found in [29].

The weak variational form of the problem of elasticity $\mathcal{WF}_{\mathrm{e}}$ is presented in [26], assuming zero body forces and the case of harmonic oscillations, for the displacement formulation where the primary dependent variable is the vector field of elastic displacements u_i^{e}. The secondary variable is the elastic stress tensor; for the relevant case of linear isotropic elasticity it can be expressed as $\sigma_{ij}^{\mathrm{e}} = \mu_{\mathrm{e}}\,(u_{i|j}^{\mathrm{e}} + u_{j|i}^{\mathrm{e}}) + \lambda_{\mathrm{e}}\,u_{k|k}^{\mathrm{e}}\,\delta_{ij}$, where the well-known Lamé coefficients: the shear modulus μ_{e} and the dilatational constant λ_{e}, appear.

The weak form of piezoelectricity $\mathcal{WF}_{\mathrm{pz}}$ is presented in [30, 26]. It can be substituted, however, with the weak form of elasticity $\mathcal{WF}_{\mathrm{e}}$ by using a simplified approach based on some analogy with the thermoelasticity or, in other words, by introducing certain equivalent initial strains. As a matter of fact, this very approach can be used for the analyses presented in this paper. This approximation is justified here because the piezoelectric inclusions affect the vibrations of a less-stiff skeleton of porous medium subjected to an acoustic wave excitation. It will be, therefore, thoroughly explained in Section 2.3 below.

Finite element methods for time-harmonic acoustics are reviewed in [31, 32]. The primary dependent variable of acoustical medium is usually the acoustic pressure. Knowing the acoustic pressure one can always determine the (complex amplitudes of) displacements, velocities and accelerations of fluid particle, using relevant formulas given, for example, in [26, 27], where the weak form $\mathcal{WF}_{\mathrm{a}}$ and the fundamental kinds of boundary conditions are also presented. The so-called non-reflecting boundary conditions (NRBC), which often play an important role, because they ensure that no (or little) spurious wave reflection occurs from the boundary, are discussed in [33].

Interface couplings between poroelastic and other media are thoroughly discussed in [29, 28, 34]. Of all these couplings, relevant for this work is the coupling between poroelastic and elastic media (and also poroelastic–acoustic coupling). For the

enhanced weak integral [28] of the mixed formulation of poroelasticity used here, the poroelastic–elastic coupling is naturally handled, i.e. the relevant interface integral is zero [28, 26].

2.2. *Biot's theory of poroelasticity*

The Biot's theory of poroelasticity [35, 11, 12] provides a biphasic model of porous media: the so-called solid phase is used to describe the behavior of the ("smeared") elastic skeleton whereas the fluid phase pertains to the fluid in the pores. Both phases are two coupled homogeneous continua. The most frequently used version of poroelasticity assumes besides that both phases are isotropic. Moreover, the fluid is modeled as inviscid, though viscous forces, are taken into account but only when modeling interaction between the fluid and the solid frame.

In the classical formulation [35, 11, 36, 12] a state of poroelastic medium is described by the displacements of solid, u_i, and fluid phase, U_i. The Biot's equations for a local dynamic equilibrium of poroelastic material link partial stress tensors associated with the skeleton particle (σ^{s}_{ij}) and the macroscopic fluid particle (σ^{f}_{ij}) with the solid and fluid macroscopic displacements. In the case of harmonic oscillations (with angular frequency ω) these equations read

$$\sigma^{\mathrm{s}}_{ij|j} + \omega^2 \tilde{\varrho}_{\mathrm{ss}}\, u_i + \omega^2 \tilde{\varrho}_{\mathrm{sf}}\, U_i = 0\,, \qquad \sigma^{\mathrm{f}}_{ij|j} + \omega^2 \tilde{\varrho}_{\mathrm{ff}}\, U_i + \omega^2 \tilde{\varrho}_{\mathrm{sf}}\, u_i = 0\,, \tag{2}$$

where the frequency-dependent effective densities, $\tilde{\varrho}_{\mathrm{ss}}$, $\tilde{\varrho}_{\mathrm{sf}}$, and $\tilde{\varrho}_{\mathrm{ff}}$, are introduced. These densities are responsible not only for the inertia of solid or fluid phase particles but also for the combined inertial and viscous coupling (interaction) of both phases. They depend on the viscous drag coefficient, $\tilde{b}$, and the normal effective densities, ϱ_{ss}, ϱ_{ff}, ϱ_{sf}. The latter quantities in turn depend on the porosity, ϕ, the tortuosity of pores, α_∞, the density of the material of skeleton, ϱ_{s}, and the density of saturating fluid, ϱ_{f}. The adequate formulas may be found in [11, 12].

The partial solid and fluid stress tensors are linearly related to the partial strain tensors prevailing in the skeleton and the interstitial fluid. This is given by the following linear and isotropic constitutive equations of the Biot's theory of poroelasticity:

$$\sigma^{\mathrm{s}}_{ij} = \mu_{\mathrm{s}}\,(u_{i|j} + u_{j|i}) + \Big(\tilde{\lambda}_{\mathrm{s}}\, u_{k|k} + \tilde{\lambda}_{\mathrm{sf}}\, U_{k|k}\Big)\delta_{ij}\,, \quad \sigma^{\mathrm{f}}_{ij} = \Big(\tilde{\lambda}_{\mathrm{f}}\, U_{k|k} + \tilde{\lambda}_{\mathrm{sf}}\, u_{k|k}\Big)\delta_{ij}\,. \tag{3}$$

Four material constants are involved here, namely μ_{s}, $\tilde{\lambda}_{\mathrm{s}}$, $\tilde{\lambda}_{\mathrm{f}}$, and $\tilde{\lambda}_{\mathrm{sf}}$. The first two of them resemble the two Lamé coefficients of isotropic elasticity. Moreover, μ_{s} is the shear modulus of the poroelastic material and consequently the shear modulus of the frame since the fluid does not contribute to the shear restoring force. The three dilatational constants, $\tilde{\lambda}_{\mathrm{s}}$, $\tilde{\lambda}_{\mathrm{f}}$ and $\tilde{\lambda}_{\mathrm{sf}}$ are frequency-dependent and are functions of K_{b}, K_{s}, and $\tilde{K}_{\mathrm{f}}$ ($\tilde{\lambda}_{\mathrm{s}}$ depends also on μ_{s}), where: K_{b} is the bulk modulus of the frame at constant pressure in the fluid, K_{s} is the bulk modulus of the elastic solid from which the frame is made, and $\tilde{K}_{\mathrm{f}}$ is the bulk modulus of the fluid in porous medium. The adequate formulas to compute the poroelastic material constants can be found in [11, 12]. Finally, the total stress tensor of poroelastic medium is defined as a simple sum of the partial, i.e. phasic, stress tensors, whereas the total displacement vector sums up porosity-dependent contributions of the displacements of both phases:

$$\sigma^{\mathrm{t}}_{ij} = \sigma^{\mathrm{s}}_{ij} + \sigma^{\mathrm{f}}_{ij}\,, \qquad u^{\mathrm{t}}_i = (1-\phi)\, u_i + \phi\, U_i\,. \tag{4}$$

The equations of equilibrium (2) together with the constitutive relations (3) form the displacement formulation of linear, isotropic poroelasticity for harmonic oscillations. Notice that the first equations from both pairs refer to the solid phase whereas the second ones to the fluid phase. Nevertheless, both phases are strongly coupled by the viscous-inertial coupling coefficient, $\tilde{\varrho}_{\mathrm{sf}}$, and the constitutive coupling constant, $\tilde{\lambda}_{\mathrm{sf}}$. In this classical formulation the unknown fields are the solid and fluid phase displacements, which means 6 degrees of freedom in every node of a three-dimensional model.

The fluid phase stress tensor can be expressed as

$$\sigma^{\mathrm{f}}_{ij} = -\phi\, p\, \delta_{ij}\,, \tag{5}$$

where p is the pressure of fluid in the pores (it should not be mistaken for the pressure of fluid phase which equals ϕp). By using this relation for the time-harmonic version of Biot's poroelasticity, the fluid phase displacements can be expressed as functions of the pressure in the pores, and thus eliminated from the equations (replaced by p); such derivation can be found in [26]. This results in the mixed displacement–pressure formulation [37, 29, 12] where the dependent variables are the three solid phase displacements and the pore-fluid pressure. Therefore, three-dimensional models have now only 4 degrees of freedom in a node.

2.3. *Approximation of piezoelectricity by initial strains*

As mentioned above, a piezoelectric domain can be often modeled as an elastic medium with some initial strain or, equivalently, subject to a specific thermal load [30]. This approximation is based on the resemblance between the thermoelastic and converse-piezoelectric constitutive equations: the stress vs. strain and voltage equation of piezoelectricity resembles the Hooke's law with initial strains (induced, for example, by a temperature field). The initial strain simulates the piezoelectric effect. Thus, in this approach the weak form of elasticity $\mathcal{WF}_{\mathrm{e}}$ is used for a piezoelectric domain with

$$\sigma^{\mathrm{e}}_{ij} = C^{\mathrm{pz}}_{ijkl}\big(S^{\mathrm{e}}_{kl} - S^{0}_{kl}\big)\,, \tag{6}$$

where $S^{\mathrm{e}}_{kl} = \frac{u^{\mathrm{e}}_{k|l} + u^{\mathrm{e}}_{k|l}}{2}$ are the elastic strains, and

$$S^{0}_{kl} = d^{\mathrm{pz}}_{ikl}\, E^{\mathrm{pz}}_{i} = -d^{\mathrm{pz}}_{ikl}\, V^{\mathrm{pz}}_{|i} \tag{7}$$

are the initial elastic strains approximating the piezoelectric effect. Furthermore, C^{pz}_{ijkl} and d^{pz}_{ikl} denote the components of the fourth-order (orthotropic or transversally isotropic) tensor of elastic material constants and the third-order tensor of piezoelectric material constants, respectively, whereas E^{pz}_{i} and V^{pz} are the electric field and electric potential; they are related by the Maxwell's law for electricity:

$$E^{\mathrm{pz}}_{i} = -V^{\mathrm{pz}}_{|i}\,. \tag{8}$$

In this approximation the electric problem is uncoupled from its mechanical counterpart and can be solved independently. Thus, the electric potential V^{pz} is found by solving the following equation of electricity (presented here with no body electric charge) in the piezoelectric domain:

$$\epsilon^{\mathrm{pz}}_{ji}\, V^{\mathrm{pz}}_{|ij} = 0\,, \tag{9}$$

where $\epsilon^{\mathrm{pz}}_{ji}$ denote the tensor of dielectric material constants, with the following electrical boundary conditions – of the Neumann and Dirichlet kind, respectively:

$$\epsilon^{\mathrm{pz}}_{ji}\, V^{\mathrm{pz}}_{|i}\, n^{\mathrm{pz}}_{j} = \hat{Q}^{\mathrm{pz}} \qquad \text{or} \qquad V^{\mathrm{pz}} = \hat{V}^{\mathrm{pz}}\,. \tag{10}$$

The Neumann condition serves for a surface electric charge $\hat{Q}^{\mathrm{pz}}$ applied on a boundary, whereas the Dirichlet condition allows to prescribe the electric potential $\hat{V}^{\mathrm{pz}}$ on a boundary. Now, the electric vector field can be computed from the Maxwell's law (8), and the "piezo-equivalent" initial strain can be found from Equation (7). In practice, for thin piezoelectric patches (of thickness t) with electrodes on the opposite sides so that the electric voltage $\Delta\hat{V}^{\mathrm{pz}}$ is applied, for example, across the x_2-direction, the electric potential field can be determined as follows: $E^{\mathrm{pz}}_{2} = \Delta\hat{V}^{\mathrm{pz}}/t$ and $E^{\mathrm{pz}}_{1} = E^{\mathrm{pz}}_{3} = 0$.

3. Acoustic absorption coefficient

The main purpose of the present analysis of poroelastic layers with solid inclusions is to assess how the passive and active inclusions can influence the acoustic absorption of layers. The acoustic absorption of a poroelastic layer fixed to a rigid wall and subject to a plane acoustic wave propagating in the air onto the layer surface at normal incidence will be computed as follows [11, 12]. First, the acoustic impedance at normal incidence is determined at the interface between the poroelastic layer and the air:

$$Z = \frac{p}{v}\,, \quad \text{where} \quad v = -v_1 = -\mathrm{j}\,\omega\, u^{\mathrm{t}}_{1} = -\mathrm{j}\,\omega\left[(1-\phi)\,u_1 + \phi\, U_1\right]. \tag{11}$$

Here, p is the (complex amplitude of) pressure, and v_1 is the (complex amplitude of) wave velocity in the x_1-direction at the layer–air interface – continuous across this boundary – which can be expressed in terms of the total normal displacements u^{t}_{1} of the surface of porous layer, or as a function of normal displacements of its solid phase and fluid phase, u_1 and U_1, respectively; (j is the imaginary unit). If the impedance is computed at the boundary of a layer of air adjacent to the porous layer, then v_1 simply equals $v^{\mathrm{a}}_{1} = \mathrm{j}\,\omega\, u^{\mathrm{a}}_{1}$, where v^{a}_{1} and u^{a}_{1} are the (complex amplitudes of) fluid particle's velocity and displacement, respectively. Now, the reflection coefficient at this point is computed as:

$$R = \frac{Z - Z_0}{Z + Z_0}\,, \tag{12}$$

where $Z_0 = \varrho_0\, c_0$ is the characteristic impedance of air; ϱ_0 is the air density and c_0 is the speed of sound. Finally, knowing the reflection coefficient, the acoustic absorption coefficient can be determined:

$$A = 1 - |R|^2\,. \tag{13}$$

This final property is real-valued, unlike the complex-valued reflection coefficient R and impedance Z.

4. Analyzed configurations

Several finite element analyses of poroelastic layers with or without solid inclusions were carried out for configurations presented in Figure 1 and 2. The configurations are two-dimensional – in the x_1x_2-plane – so an adequate extrusion in the x_3-direction – normal to the plane of the drawing – is assumed. Nevertheless, this approach should also give good predictions for similar three-dimensional configurations of sufficient regularity. The total thickness of layer in each configuration is always 16 mm. At $x_1 = 0$ mm the layer is fixed to a rigid wall whereas at $x_1 = 16$ mm the plane harmonic acoustic wave impinges on the surface of the poroelastic layer. The following six configurations were analyzed (see Figure 1):

NoInc – a simple macro-homogeneous layer of porous foam with **no inclusions**;

Al-S – two layers of porous foam linked by a **septum** of 0.2 mm-thick **aluminum** foil;

Al-9 – a layer of porous foam with densely-set **9 mm**-wide stripes of 0.2 mm-thick **aluminum** foil;

Al-4 – a layer of porous foam with loosely-set **4 mm**-wide stripes of 0.2 mm-thick **aluminum** foil;

I-sh – a layer of porous foam with parallel **I-shaped** inclusions fixed to a rigid wall;

T-sh – a layer of porous foam with **T-shaped** inclusions made up of stripes of 0.2 mm-thick aluminum foil fixed to active elements made up from PZT ceramic.

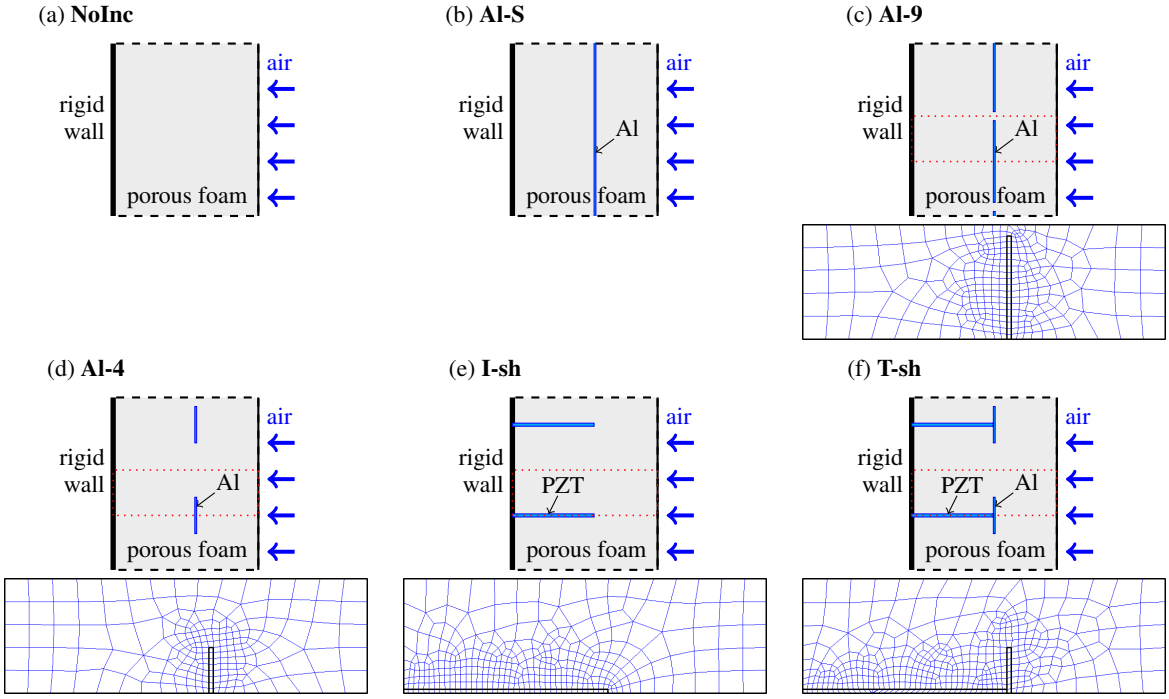

Figure 1: Analyzed configurations of porous composites and the corresponding finite-element meshes of the representative subdomain. The total thickness of each composite is 16 mm (see also Figure 2 for other dimensions and the axes). The configurations are layers of poroelastic foam and differ only by the embedded inclusions, as follows: (a) **NoInc** – no inclusions, (b) **Al-S** – a septum of aluminum foil, (c) **Al-9** – 9 mm-wide stripes of aluminum foil, (d) **Al-4** – 4 mm-wide stripes of aluminum foil, (e) **I-sh** – fixed I-shaped inclusions, (f) **T-sh** – active T-shaped inclusions.

Table 1: Poroelastic properties of two polyurethane foams.

		Foam A	Foam B
porosity	ϕ	0.97	0.99
tortuosity	α_∞	2.52	1.98
flow resistivity	σ	87 kN s/m^4	65 kN s/m^4
characteristic dimension of pores:			
– for viscous forces	Λ	$37 \cdot 10^{-6}$m	$37 \cdot 10^{-6}$m
– for thermal forces	Λ'	$119 \cdot 10^{-6}$m	$121 \cdot 10^{-6}$m
solid-phase mass density	ϱ_{sph}	31 kg/m^3	16 kg/m^3
shear modulus	μ_{s}	$55(1+\vartheta\text{j})$ kPa	$18(1+\vartheta\text{j})$ kPa
loss factor	ϑ	0.055	0.1
bulk Poisson's ratio	ν_{b}	0.3	0.3

Two high-porosity polyurethane foams (termed A and B) were considered for these configurations. Poroelastic data for these foams are given in Table 1. The first four configurations are passive, while the configurations I-sh and T-sh have active elements made up of piezoelectric ceramic whose elastic and piezoelectric material constants are given in Table 2, where it is assumed that the material is polarized along the x_2-axis; its mass density is 7500 kg/m^3, and the relative dielectric constants in the absence of stress are $\epsilon^{\text{pz}}_{11} = \epsilon^{\text{pz}}_{33} = 3130$, $\epsilon^{\text{pz}}_{22} = 3400$. The results of the acoustic absorption in passive and active states will be presented for the last configuration with T-shaped inclusions (see Figure 2). Notice that this configuration is, in fact, a combination of the configurations Al-4 and I-sh.

As mentioned above, the problem is modeled as two-dimensional, in the x_1x_2-plane. Moreover, the symmetry (regularity along the x_2-axis) makes it possible to model only a rectangular domain ABCD of the layer comprising only a half of one inclusion (see Figures 1 and 2) by applying proper boundary conditions, namely, by blocking the normal displacements on

Table 2: Elastic and piezoelectric material constants constants: C^{pz}_{ijkl} [GPa] and d^{pz}_{ikl} [10^{-12} m/V], respectively – for PZT ceramic (polarized along the x_2-axis).

$C^{pz}_{ijkl}/[\text{GPa}]$

	$kl=11$	$kl=22$	$kl=33$	$kl=23$	$kl=31$	$kl=12$
$ij=11$	127	84.7	80.2	0	0	0
$ij=22$	84.7	117	84.7	0	0	0
$ij=33$	80.2	84.7	127	0	0	0
$ij=23$	0	0	0	23.0	0	0
$ij=31$	0	0	0	0	23.5	0
$ij=12$	0	0	0	0	0	23.0

$d^{pz}_{ikl}/(10^{-12}[\text{m/V}])$

	$kl=11$	$kl=22$	$kl=33$	$kl=23$	$kl=31$	$kl=12$
$i=1$	0	0	0	0	0	741
$i=2$	-274	593	-274	0	0	0
$i=3$	0	0	0	741	0	0

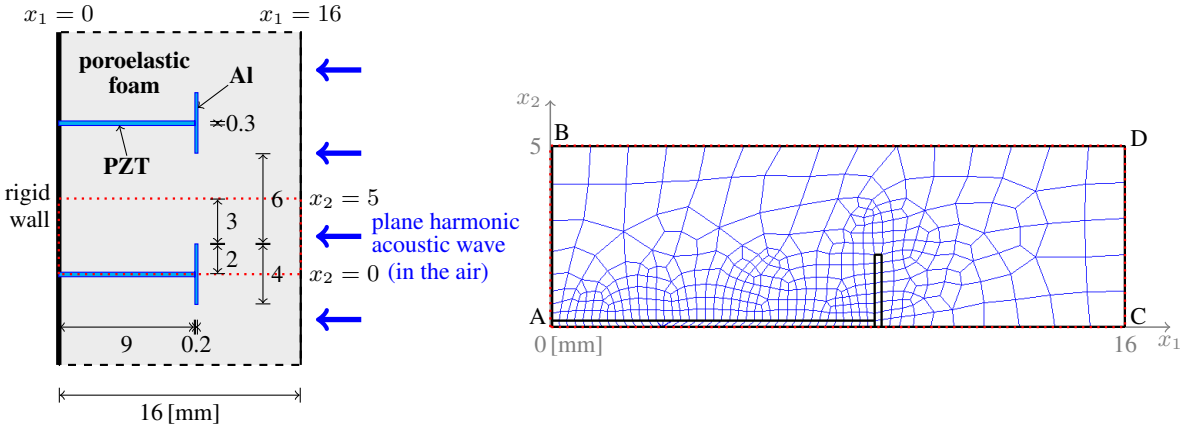

Figure 2: Detail of the T-sh active composite configuration and the finite-element mesh of the modeled representative subdomain.

the two lateral edges – AC and BD – of the modeled rectangular domain (i.e., $u_2 = 0$ and $U_2 = 0$ on AC and BD). For some configurations the corresponding finite-element meshes are given, see Figure 1. Such meshes are not presented for the configurations NoInc and Al-S since for such regular single- and multi-layered media planar analytical solutions can be used; as a matter of fact, the finite-element analyses were also performed for these two cases and gave the same results as the corresponding one-dimensional analytical solutions. All necessary dimensions for the active composite T-sh are given in Figure 2, where the finite-element mesh of the representative modeled subdomain ABCD is also shown. Relevant dimensions from this figure are also valid for other configurations.

The analysis consisted in determining the acoustic absorption of the poroelastic composites. To this end, the results of finite-element analysis – especially, the total normal displacements u_1^t at the layer's surface – were used by the analytical formulas for the impedance, the reflection and absorption coefficients (see Section 3). These formulas result from a one-dimensional analysis of the plane wave propagation which is slightly violated if solid inclusions are present. Therefore, the absorption coefficient was computed at two points of the layer surface: at point C ($x_2 = 0$ mm) and point D ($x_2 = 5$ mm) – see Figure 2 – and the average was taken from the two values. This approach is validated in Appendix at the end of this paper. The averaging approach can also be used for the case when a *thin* adjacent layer of fluid is modeled (for example, in case of active analysis) in order to apply the high-order non-reflecting boundary scheme for time-harmonic waves [38].

5. Acoustic absorption of the passive poroelastic composites

Figure 3 presents the acoustic absorption of passive poroelastic composites – curve (b)-(f) – compared to the absorption of the porous layer of the same thickness but without inclusions – curve (a); the porous material is foam A with properties presented in Table 1. The upper graph shows the absorption curves for the layer with a continuous septum made up of 0.2 mm-thick aluminum foil – curves (b), and for the layers with aluminum stripes, 9 mm or 4 mm wide, made up of the same foil – curves (c) and (d), respectively. The continuous septum deteriorates generally the acoustic absorption, however, such composite exhibits a great performance around a particular single frequency (i.e., at 1000 Hz). The aluminum stripes improve the absorption in some

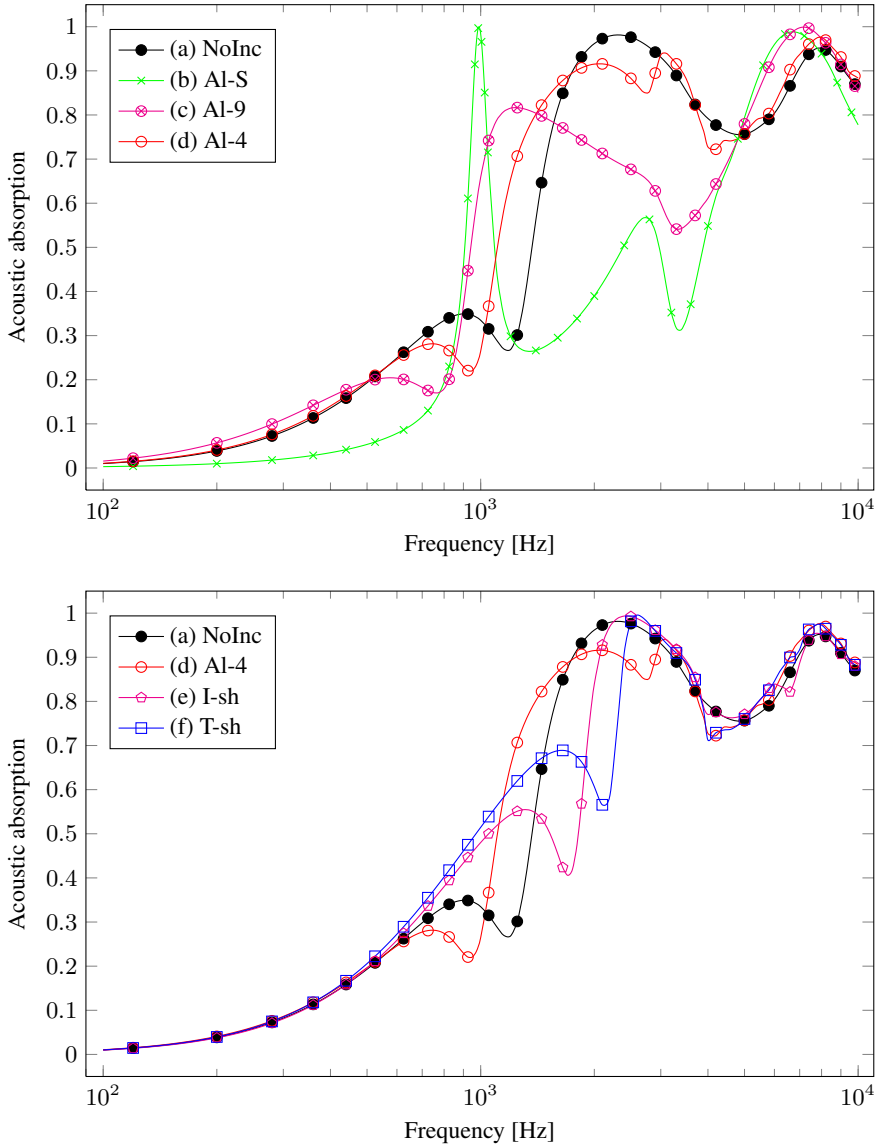

Figure 3: Passive absorption curves for the porous composite/layer made up of foam A.

frequency range but deteriorate it in another. The lower graph of Figure 3 shows the acoustic absorption of the layer with no inclusions – curve (a) – compared with the absorption curves of three composites: with 4 mm-wide aluminum stripes – curve (d), with fixed (passive) I-shaped inclusions – curve (e), and with complete (passive) T-shaped inclusions – curve (f). For the lowest frequencies (up to 600 Hz) there is no difference between the curves: the absorption is poor since not much can be achieved with layers only 16 mm thick. Between 600 to 3000 Hz the absorption of composites with inclusions is better in some range of frequencies and worse in another range. Above 2100 Hz – for I-sh, 2500 Hz – for T-sh, or 3000 Hz – for Al-4, the absorption curves of composites are similar to the absorption curve of macro-homogeneous layer.

Similar analysis was carried out for the layer and composites made up of foam B (see Table 1 for the poroelastic data). The results of the acoustic absorption are presented in Figure 4 and since the thickness of layers, inner geometry and material of inclusions are the same as for the composites made up of foam A, the conclusions are similar. The composite Al-S (with the continuous aluminum septum) has the worst absorption with the exception of a narrow range around 800 Hz where locally the absorption approaches 1 – see curve (b) in Figure 4. The composite Al-9 has the best absorption between 700 HZ and 1800 Hz but worse for other frequencies – see curve (c). There is no significant difference in the absorption curves of the macro-homogeneous layer and the porous composites Al-4, I-sh, and T-sh at frequencies lower than 500 Hz or higher than 2700 Hz – compare curves (d), (e), and (f) in Figure 4, respectively. In between, the composites have better performance in some range of frequencies and worse in another range.

A drop in acoustic absorption observed in the medium frequency range, namely, closely to 1.2 kHz for the foam A (without inclusions) – curve (a) in Figure 3, and around 0.9 kHz for the foam B – curve (a) in Figure 4, results from the first resonance of the skeleton (or the solid-borne wave), which is – for layers stuck to a rigid wall – the *quarter-wavelength* resonance [39]. In the vicinity of this resonance frequency f_r, the frame stiffness can have a great influence on the absorption coefficient [39, 40]. Air

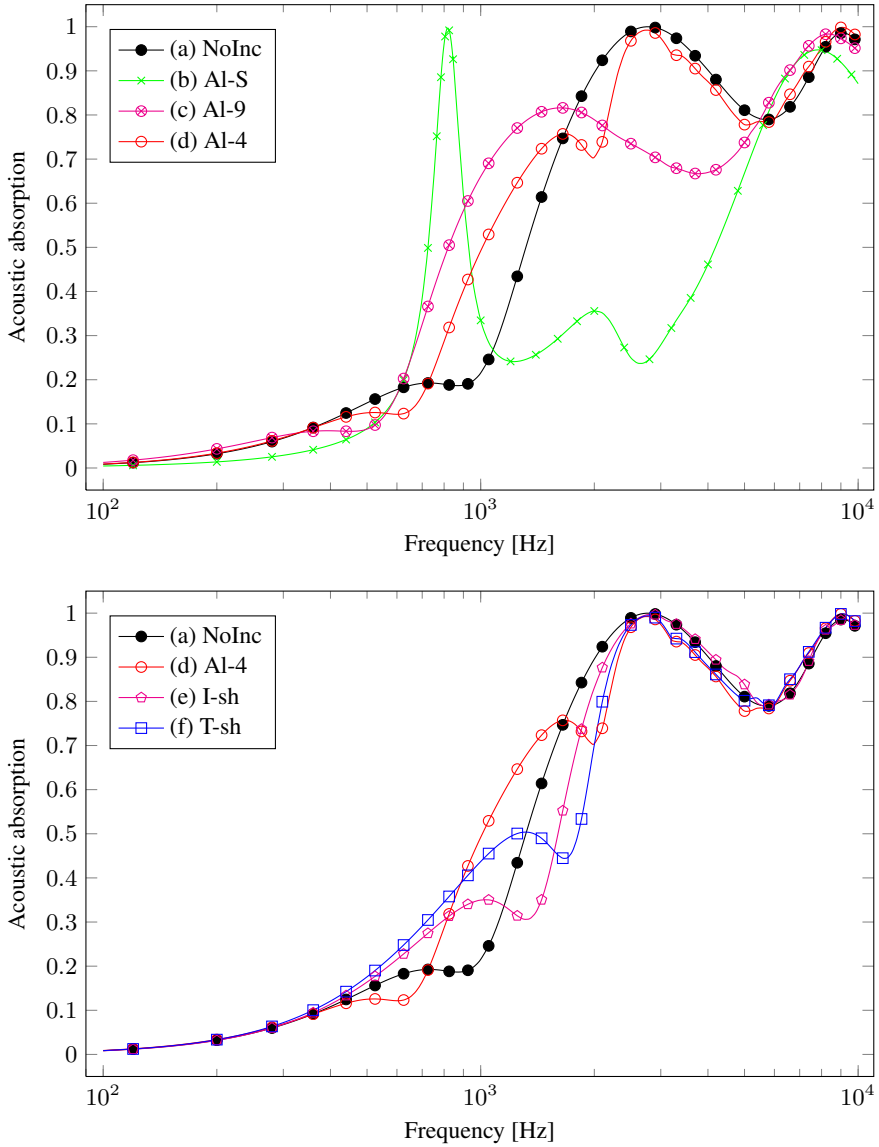

Figure 4: Passive absorption curves for the porous composite/layer made up of foam B.

being much lighter, and having a much smaller bulk modulus than the skeleton [39], permits to estimate this frequency by simply considering the properties of the frame *in vacuo*, as follows [39, 40]:

$$f_{\mathrm{r}} \approx \frac{1}{4\,L}\sqrt{\frac{P_{\mathrm{sph}}}{\rho_{\mathrm{sph}}}} \tag{14}$$

where L is the thickness of layer (here, $L = 16\,\mathrm{mm}$), ρ_{sph} is the solid phase density (i.e., the density of the porous material in a vacuum), and

$$P_{\mathrm{sph}} = \frac{2\,(1-\nu_{\mathrm{b}})}{1-2\,\nu_{\mathrm{b}}}\,\mathrm{Re}\,\mu_{\mathrm{s}} \tag{15}$$

is the P-wave modulus of solid phase. For the foam A: $P_{\mathrm{sph}} = 192.5\,\mathrm{kPa}$ and the estimation of quarter-wavelength resonance for the layer made up of this foam is $f_{\mathrm{r}} \approx 1.23\,\mathrm{kHz}$, whereas for the foam B: $P_{\mathrm{sph}} = 63\,\mathrm{kPa}$ and $f_{\mathrm{r}} \approx 0.98\,\mathrm{kHz}$. These values agree rather well with the frequencies of the observed above drops in the absorption curves. Now, from Figures 3 and 4 it can be noticed that the inclusions Al-9 and Al-4 lower this frequency, while I-sh and T-sh increase it. This is because the inclusions Al-9 and Al-4, being loosely-set, add (mainly) some mass, whereas the inclusions I-sh and T-sh are fixed to the backing wall, and so they add stiffness to porous layers.

The final general conclusion is that the T-shaped inclusions change the absorption in a range of medium frequencies: they improve it for the lower-frequency part of this range (where the absorption is weak) and deteriorate it at higher frequencies (where the absorption is better altogether). Still, an active approach should be tried to get the best performance in the widest possible frequency range.

Remember that all the absorption curves presented above (and in the next Section) were calculated as the average of two results of acoustic absorption computed at points C and D (see Figure 2). The validity of such averaging approach is given in Appendix.

6. Active improvement of the acoustic absorption

The general idea of active improvement of the acoustic absorption of poroelastic composites can be explained as follows. A harmonic acoustic wave propagates in air and impinges on the surface of a poroelastic layer (or composite). Higher frequency waves can be well absorbed by the layer but at lower frequencies the acoustic absorption of thin layers is very poor. Now, the acoustic wave continues to propagate in the porous medium and is reflected by the rigid wall. In fact, there are three waves: a fast longitudinal (or compressional) wave and a shear (or transverse) wave, both originating mainly from the elastic solid of skeleton, and a slow longitudinal (or compressional) fluid-borne wave. At lower frequencies the solid–fluid coupling occurs, so that the vibrations of elastic skeleton interact with the vibrations of air in the pores. Because of this coupling the acoustic absorption may be actively modified by affecting the vibrations of the elastic skeleton. Since the traction between the air and the solid frame of porous medium is the main absorption mechanism, the elastic skeleton is actively vibrated in order to adapt and improve the dissipative interaction of the skeleton and air in the pores. To this end, active inclusions are embedded into the porous layer and an appropriate harmonic excitation signal is applied to the electrodes of the piezoelectric parts of these inclusions. The results presented in this Section show the feasibility of this approach.

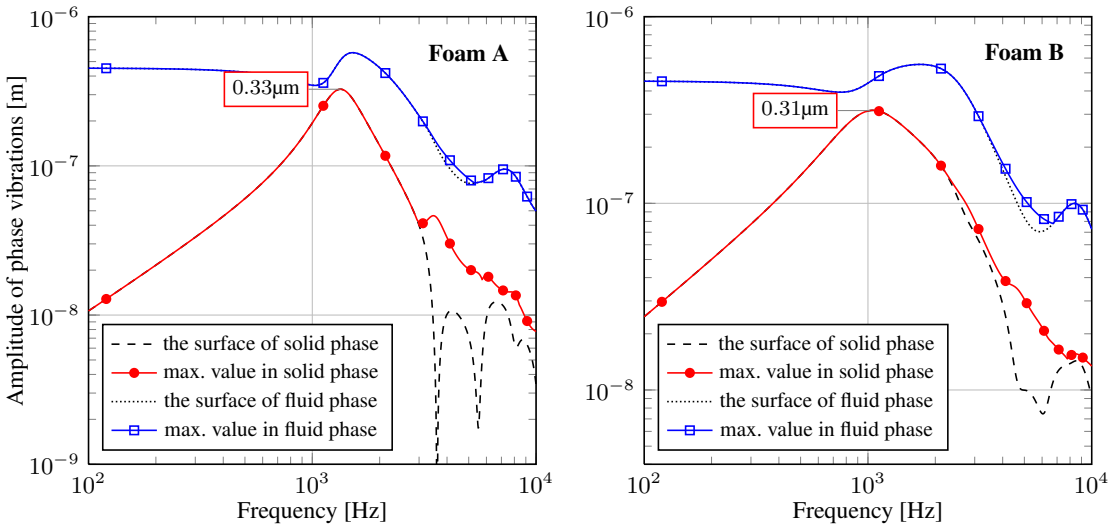

Figure 5: The amplitudes of vibrations of the solid and fluid phases of the 16 mm-thick porous layers subject to the harmonic pressure excitation with the amplitude $p_0 = 2\sqrt{2}$ Pa.

Figure 5 shows the amplitudes of vibrations of the solid phase of porous foams with no inclusions. Additionally, the amplitude curves for the fluid phase are also shown. All the curves are calculated for the 16 mm-thick layers of the foams subject to the harmonic excitation by the acoustic pressure of amplitude $p_0 = 2\sqrt{2}$ Pa, which means that the root-mean-square pressure equals $p_{\text{rms}} = 2$ Pa and that gives the sound pressure level of 100 dB (with the reference pressure $p_{\text{ref}} = 2 \times 10^{-5}$ Pa). The amplitudes for the solid phase indicate the order of maximal displacements of the elastic skeleton. For both foams, two curves are actually plotted for each of the two phases, namely:

- the curve of the amplitude of vibrations at the free interface CD (see Figure 2 or A1) between the porous layer and the air, that is at $x_1 = 16$ mm,
- the curve of the maximal amplitude for $x_1 \in [0\,\text{mm}, 16\,\text{mm}]$, that is for the whole domain of the porous layer.

It should be noticed for the solid phase curves, that at lower frequencies, that is: under 3100 Hz for foam A, or 2300 Hz for foam B, both curves are the same since the maximal amplitudes of layer vibrations are at the free interface. An important observation is that for the pressure level of 100 dB the maximal amplitudes of vibrations of the elastic skeletons of both porous layers slightly exceed 0.3×10^{-6} m. The order of magnitude of the amplitudes of vibrations of the fluid phase is bigger. One should remember, however, that the vibrations of elastic skeleton are strongly coupled (at lower frequencies) with the vibrations of the air in the pores. To investigate the potential of this interaction is an important purpose of this paper.

As explained previously the fixed parts of the T-shaped inclusions can be active – they are thin patches of piezoelectric ceramic PZT (see Table 2), through-thickness polarized, 9 mm long and 0.3 mm thick (see Figure 2). It was estimated analytically and checked by FE analysis that they would stretch more than 0.008×10^{-6} m/V, which means that, for example, voltage of 20 V

applied to the electrodes of the piezo-element would extend it for more than 0.16×10^{-6} m. It means that a harmonic signal of similar voltage amplitude should vibrate the elastic skeleton up to the amplitudes of the same magnitude as the amplitudes of vibrations caused by a harmonic noise of 100 dB SPL, see Figures 5. Thus, the active inclusions may affect the vibrations of elastic skeleton in order to improve the acoustic absorption of the active poroelastic composite. The results presented below prove the feasibility of this assumption.

Figure 6 shows passive and active absorption curves for the foam-A layer without inclusions and composite with T-shaped inclusions in the frequency range from 100 to 2100 Hz. Similarly, Figure 7 shows absorption curves for the foam-B layer and composite in the frequency range from 100 to 2600 Hz. Additionally, the acoustic absorption curves for layers made up of *hypothetic* porous materials with rigid frame are shown to point out that some improvement of absorption at lower frequencies may be achieved by simply making the skeleton rigid; they were computed using the so-called fluid-equivalent model [12] with all relevant porous parameters taken as for the considered (poroelastic) polyurethane foams. One must remember, however, that in practice, one cannot so easily stiffen the frame and the rigid-frame assumption is valid for many materials *only* at higher frequencies. Therefore, the rigid-frame curves presented here are *not* valid (due to significant skeleton motion at medium and lower frequencies), and should only give an insight on how a damping of the frame vibrations may contribute to absorption enhancement. However, the idea of this work is to show that instead of simply damping the skeleton vibrations, some advantageous vibrations can be induced in order to increase the dissipation due to relative fluid-skeleton motion, and achieve in that way better performance in the whole frequency range – as shown by the *active* absorption curves in Figures 6 and 7.

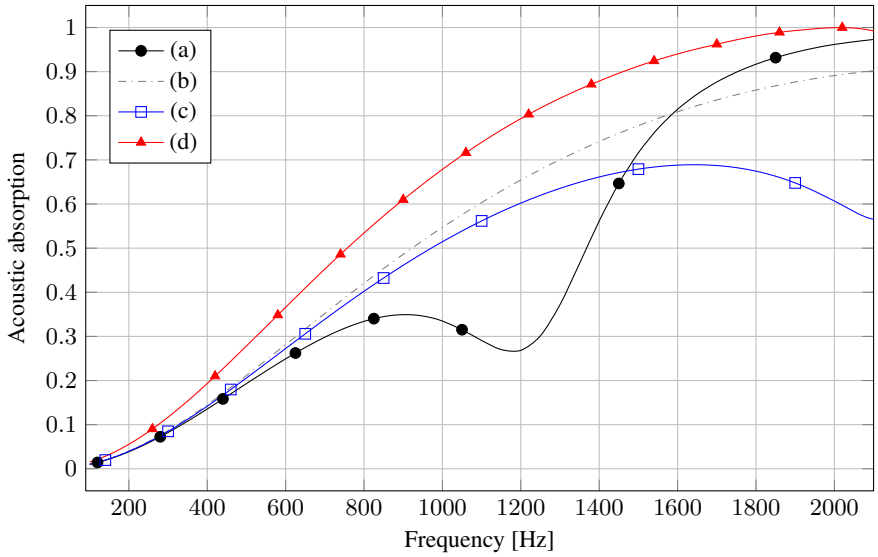

Figure 6: Absorption curves for the foam A: (a) the poroelastic layer with no inclusions, (b) the hypothetic rigid-frame layer, (c) the poroelastic composite with T-shaped inclusions in passive state, (d) the same composite with actively improved absorption.

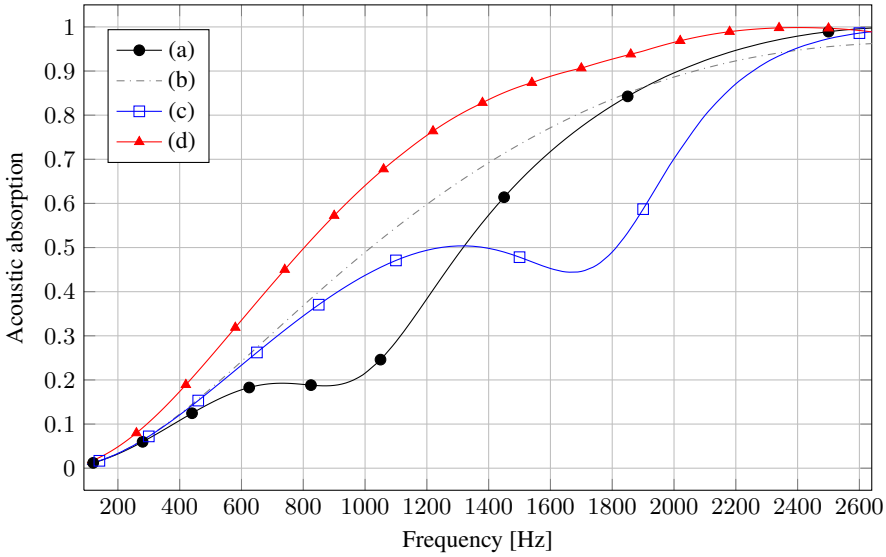

Figure 7: Absorption curves for the foam B: (a) the poroelastic layer with no inclusions, (b) the hypothetic rigid-frame layer, (c) the poroelastic composite with T-shaped inclusions in passive state, (d) the same composite with actively improved absorption.

As mentioned above, for the active absorption, a harmonic excitation signal is applied to the electrodes of the piezoelectric parts of the T-shaped inclusions. The frequency of the signal equals to the frequency of the harmonic acoustic wave of 100 dB SPL, which at the same time impinges the surface of the composite. For the whole considered frequency range, the voltage amplitude is constant: it is 18 V for the foam-A composite and 24 V for the foam-B composite. Such very moderate voltages of active signals were used to be sure that the material and kinematic linearity assumptions are not violated. The extensions produced by these voltage amplitudes are similar to the displacements of skeleton produced by the impinging waves of 100 dB SPL and smaller than the characteristic displacements of fluid phase (cf. also Figures 10 and 11 below, for the resultant amplitudes of vibrations of both phases across the thickness of layer). Moreover, they are hundred times smaller than the characteristic dimensions of pores and so the induced deformations should be small enough to ensure that the behavior is purely linear, that is, for example, that the pores are always of similar shape and size. It was checked that even more improvement in absorption is still possible at lower frequencies when increasing the voltage amplitudes, however, too high voltage amplitudes might in reality stretch the skeleton so that the pores are distorted which by any means cannot be grasped by the applied modeling and so the results obtained in that way cannot be valid.

Although the voltage signals for active enhancement of absorption have constant, that is, frequency-independent, amplitudes, the phase-shifts of these signals depend on frequency. In order to find some advantageous phase-shifts – with respect to the phase of impinging acoustic wave – calculations were carried out and optimal values of phase-shifts were selected for successive frequency ranges by comparing the acquired absorption curves. For example, Figure 8 presents active absorption curves for the foam-B composite obtained from computations realized by successively increasing the value of phase shift by 10°, starting from 0° – which is the case of *no phase shift* between the mutually-applied electric and acoustic excitations – up to 100° – where it can be observed that the absorption curve is nowhere superior from the previous results and it certainly marks a tendency. In that way, the optimal absorption curve – (d) in Figure 7 and the (red) thick-dotted curve in Figure 8 – can be found as a combination of the best results achieved in successive frequency ranges, namely: 20° is quite an optimal phase shift in the frequency range below 1.2 kHz, then, in the range from 1.2 kHz to 1.8 kHz, it must be gradually increased from 20° to 70°, and remain 70° till 2.6 kHz, which marks the end of the frequency range considered here for active enhancement of acoustic absorption. Notice, however, that almost the same absorption curve is obtained from the three curves distinguished in Figure 8, that is, for phase-shifts: 20° below 1.3 kHz, 50° in the range from 1.3 kHz to 1.7 kHz, and 70° above 1.7 kHz.

Figure 9 presents a comparison between the relative motions obtained for: the porous layer without inclusions, the porous composite with passive inclusions, and this composite with "optimally working" active inclusions, all with the same scaling factor. The porous material is foam B, the excitation is a harmonic wave of frequency 900 Hz and SPL of 100 dB, and the active excitation is realized by a voltage signal of the same frequency and optimally chosen phase shift of 20°, with the amplitude of 24 V. Figure 9 shows the displacements (deformation) of solid phase (represented by the wireframed domain) relatively to the displacements of fluid phase (represented by the arrows) for the three cases mentioned above, at phase angles changed every 45°. Additionally, Figures 10 and 11 compare the relative motions of both phases in a more quantitative manner: by showing the amplitudes and phase-angles of vibrations inside the porous foam B; in case of the composites, it is along the symmetry line BD, for $x_2 = 5$ mm, (see Figure 2), where the only non-zero components are those along the x_1-axis, that is, u_1 for the solid phase and U_1 for the fluid phase. Figure 10 shows the amplitude and phase-angle curves obtained from the frequency analysis at 900 Hz, whereas similar results in Figure 11 are for 1600 Hz.

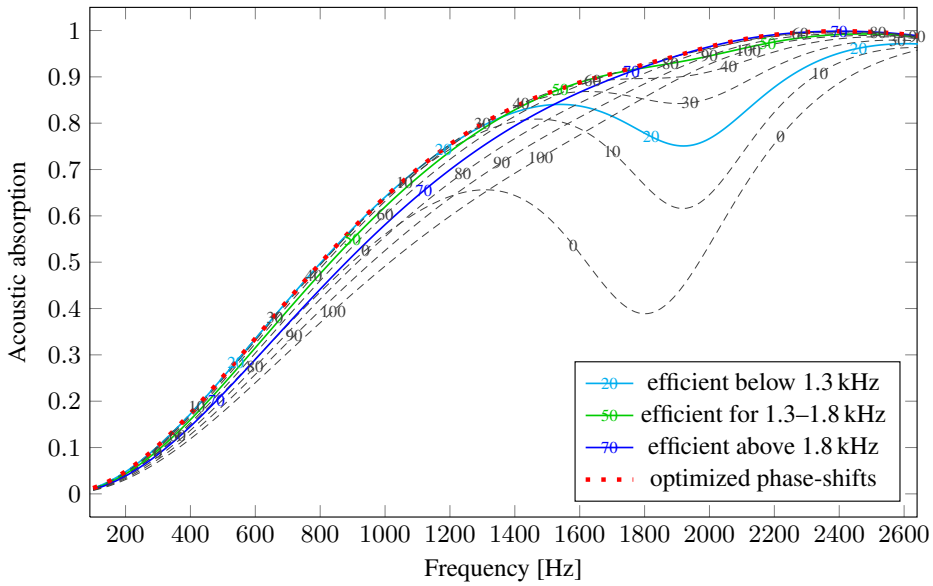

Figure 8: Active absorption curves for the foam-B composite obtained for the voltage amplitude of 24 V and phase-shifts from 0° to 100°, and the absorption curve with optimized phase-shifts.

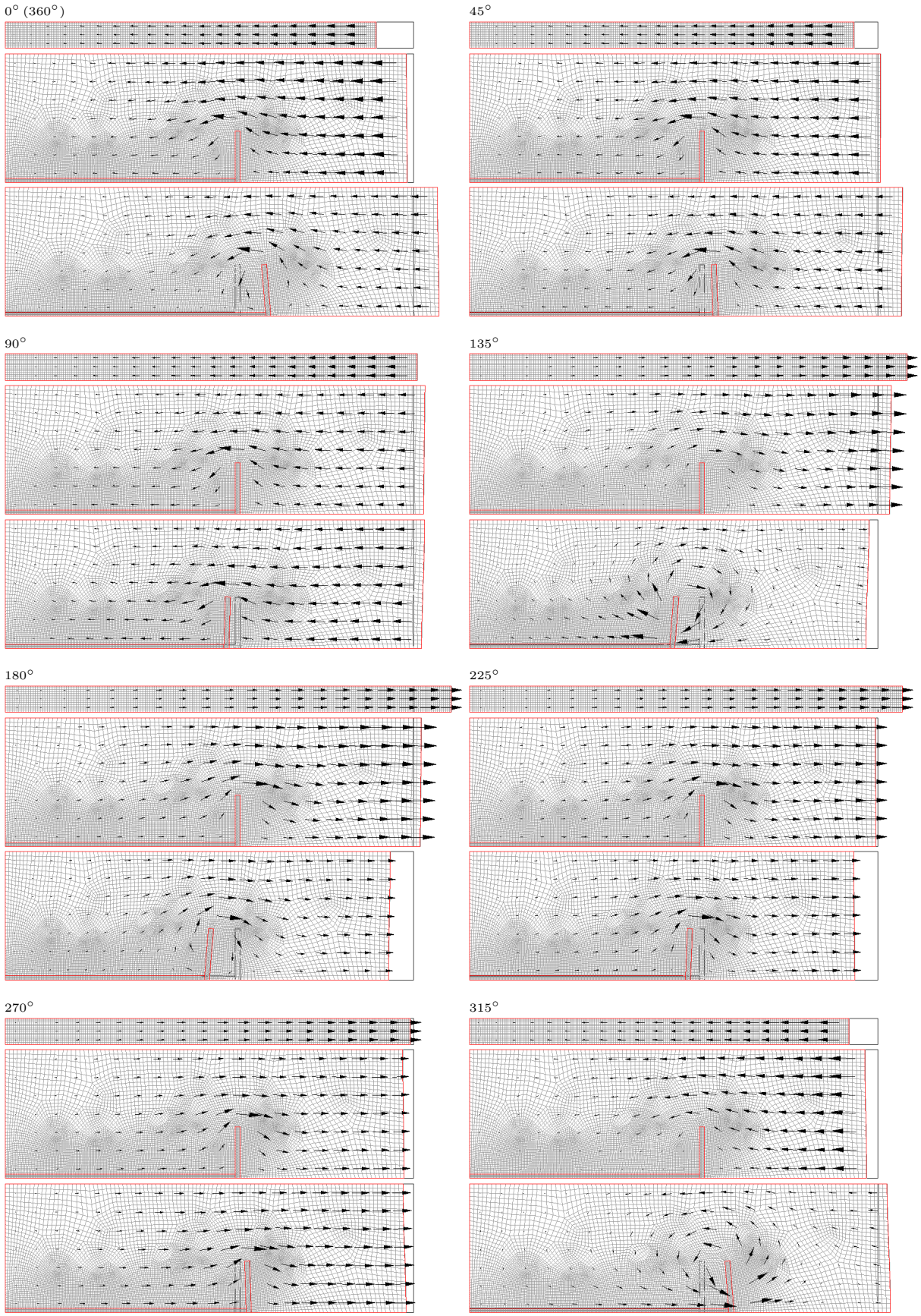

Figure 9: Relative motion – shown at successive phase angles – of solid phase (wireframe) and fluid phase (arrows) of the foam-B layer, passive composite, and active composite – top, middle, and bottom graphs, respectively, at each phase angle – for the 900 Hz excitations.

It can be shown that for high-porosity foams the imaginary part of the fluid phase displacement seems to be "responsible" for absorption, which is increased if the phase angle of the fluid vibrations is closer to 90°. This is well illustrated in Figures 10 and 11: compare curves (b), (d), and (f) in both Figures, with regard to the relevant absorption values read from Figure 7.

Another general observation, relevant for both frequency analyses and clearly visible in Figures 10 and 11, is that the amplitudes of vibrations of the fluid phase are larger that the solid phase amplitudes. However, for the layer without inclusions at 900 Hz the solid phase vibrations – curve (a) in Figure 10(left) – are comparable in amplitude to the fluid phase – curve (b); moreover, the phase angles for the skeleton and the fluid are very close to each other – compare curves (a) and (b), respectively, in Figure 10(right). That illustrates the effect of frame resonance discussed in Section 5, and the drop in acoustic absorption (see curve (a) in Figures 7 or 4) due to the in-phase motion of the frame with the fluid. This effect is weakened when the frame is stiffened by the embedded inclusions: for the passive composite at 900 Hz the solid phase vibrations – curve (c) in Figure 10(left) – are smaller, and moreover, the phase difference between the solid skeleton and the fluid – respectively, curves (c) and (d) in Figure 10(right) – is now increased, which improves the energy dissipation. However, even more enhancement in absorption is achieved when the active inclusions properly vibrate the skeleton, so that the phase angle difference between both phases is

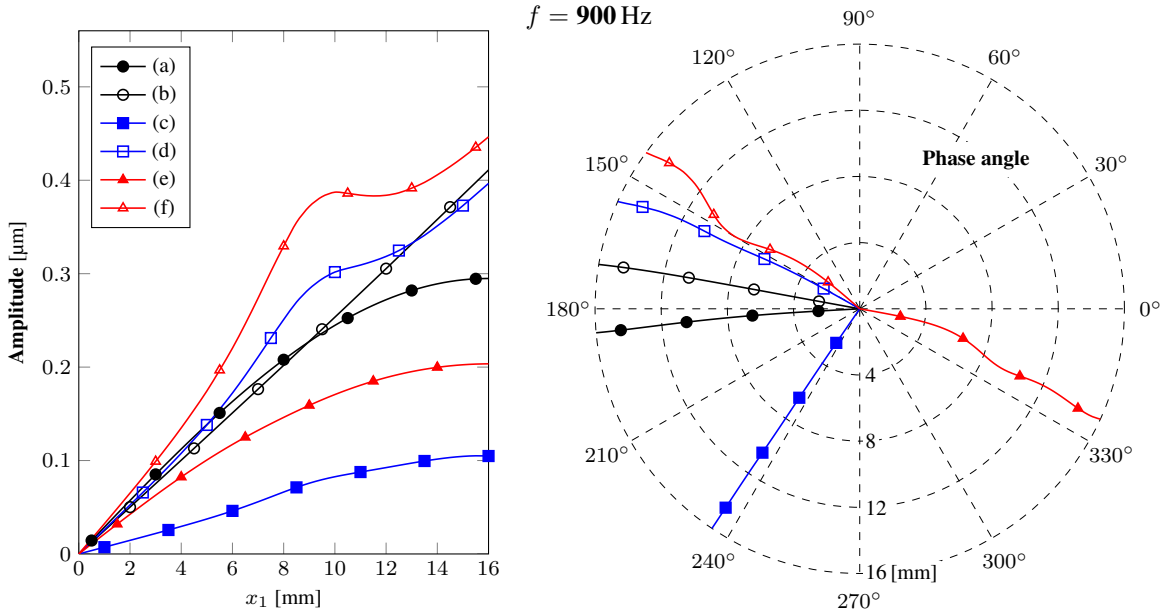

Figure 10: The amplitudes and phase angles of vibrations at 900 Hz – on the symmetry line BD (in case of the composites, see Figure 2) – of the solid phase (a,c,e) and the fluid phase (b,d,f) of foam B for: (a,b) the poroelastic layer with no inclusions, (c,d) the poroelastic composite with T-shaped inclusions in passive state, (e,f) the same composite with actively enhanced absorption.

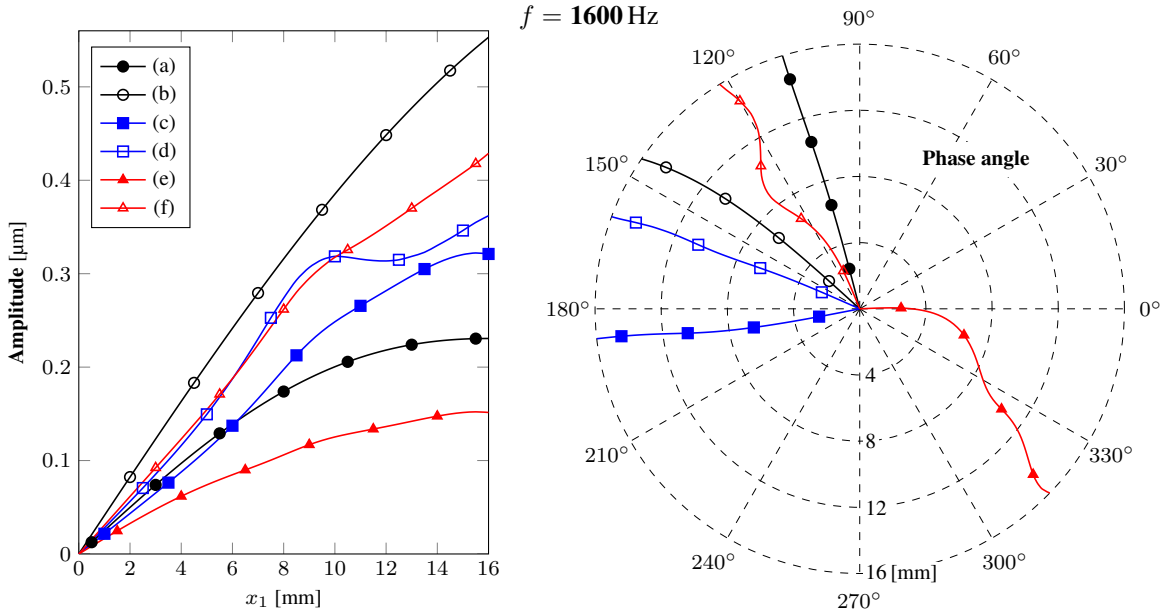

Figure 11: The amplitudes and phase angles of vibrations at 1600 Hz – see Figure 10 for additional explanations.

nearly 180° – compare, respectively, curves (e) and (f) in Figure 10(right). A similar discussion can be done for the frequency analysis carried out for 1600 Hz. Notice, however, that at 1600 Hz the acoustic absorption of the passive composite is inferior to the absorption of the layer without inclusions (compare curves (c) and (a) in Figure 7). This seems to be reflected by the curves shown in Figure 11: the amplitudes and phase angles of vibrations in the passive composite – curves (c) for the solid phase and (d) for the fluid phase – are rather similar for both phases, which means that the energy dissipation is not very effective. In case of the layer without inclusions the phase angle difference is not large either, yet the amplitudes are quite different, and the phase angle of the fluid is closer to 90° – see curves (a) and (b) in Figure 11. Obviously, approximately 160° of phase angle difference between the vibrations of the solid frame and porefluid achieved in case of the active composite – compare curves (e) and (f) in Figure 11(right) – gains an excellent acoustic absorption coefficient (see curve (d) in Figure 7).

When analyzing the results shown in Figures 10 or 11, one must remember, however, that in case of the composites the motion is two-dimensional, which is well depicted by graphs in Figure 9 for the frequency of 900 Hz. Thus, the interaction of both phases is certainly more complicated, and might not be fully described on the basis of the curves presented in Figure 10. In case of the active composite, for example, a significant rotational movement in the fluid phase occurs around the tip of the moving inclusion, which is clearly visible in Figure 9, especially, at the phase angles of 135° and 315°. Such motion should certainly play some role in energy dissipation. Nevertheless, all the conclusions presented above are confirmed by Figure 9: at 900 Hz the relative motions are roughly similar for the case of porous layer without inclusions and the passive composite, though the solid phase vibrations in the composite are reduced by the presence of stiff inclusion. In the case of the active composite, the motion of solid phase is distinctly different from the two passive cases: the deformed solid frame is first extruded *against* the fluid – this is also clearly indicated by nearly 180° of phase difference shown by curves (e) and (f) in Figure 10(right); then, the frame is driven back in order to roughly follow, though with some delay, the motion of the fluid. Thus, the dissipation is not achieved by the generation of attenuating counter-waves in the air but rather by an improvement of dissipative mechanism of viscous traction forces between the solid skeleton and air in the pores. Finally, it should be noticed that the relative optimal motion for better dissipation should depend on some global parameters of porous medium, like tortuosity or characteristic dimensions of pores, which are "responsible" for the dissipation effects.

7. Conclusions

Thin layers of porous foams with active and passive inclusions were modeled and analyzed in order to asses their acoustic absorption. The porous foams were modeled using the advanced biphasic Biot's theory of poroelasticity because the elastic vibrations of skeleton cannot be neglected for these foams and actually play an important role in the problem.

The proposed T-shaped inclusions (in the passive state) improve the acoustic absorption of a thin porous layer in some range of lower frequencies (where the absorption is poor), but can decrease it in another range of higher frequencies (where altogether, the absorption is better). Similar statement is also valid for stripes of aluminum foil embedded inside the porous layer. For the lowest frequencies and above some high frequency there is no difference in the absorption curves of the porous layer with or without inclusions.

The actuators in the form of thin patches of PZT ceramic are able to extend enough to affect the vibrations of the elastic skeleton of polyurethane foams induced by acoustic waves of significant amplitudes. This influence is better for the proposed T-shaped inclusions. At lower frequencies the coupling between the solid and fluid phases is strong enough to allow for the exploitation by the proposed active approach: electric signals with moderate amplitudes applied to the active piezoelectric parts of T-shaped inclusions, give significant improvement of the acoustic absorption of porous composites subject to the acoustic wave excitation of 100 dB SPL. The phase-shifts of the optimal signals depend on frequency. The enhancement in absorption is not achieved by the generation of attenuating counter-waves in the air but by increasing the dissipative mechanism of viscous traction forces between the solid skeleton and air in the pores. The analysis of powers dissipated in porous material [41, 42] may be used to confirm the significance of information read from the absorption curves.

Finally, it should be noticed that the active-passive inclusions should be eventually designed with respect to more than one objective, for example, as ribs increasing structural stiffness and acoustic performance of a thin acoustically-absorbing composite.

Acknowledgements

Financial support of the Foundation for Polish Science Team Programme co-financed by the EU European Regional Development Fund Operational Programme "Innovative Economy 2007-2013": Project "Smart Technologies for Safety Engineering – SMART and SAFE", No. TEAM/2008-1/4, and Project "Modern Material Technologies in Aerospace Industry", No. POIG.01.01.02-00-015/08, is gratefully acknowledged.

Appendix A. Validation of the averaging approach to absorption calculation

The formulas in Section 3 assume the plane wave propagation. This assumption is slightly violated when solid inclusions are present in porous layer. Therefore, the absorption curves presented in the paper were calculated as the arithmetic average of two values of acoustic absorption computed at points C and D (see Figure 2). Here, it will be shown that in some relevant frequency

range the two values are very similar, indeed, and so in general, the average curve gives a correct result. Moreover, the validity of the average curve is confirmed by the analysis performed using an extended model, shown in Figure A1, which contains an adjacent layer of air, sufficiently thick, so that the wave would become plane on the layer's boundary EF. Thus, the averaging approach may be considered as an effective method to achieve correct results.

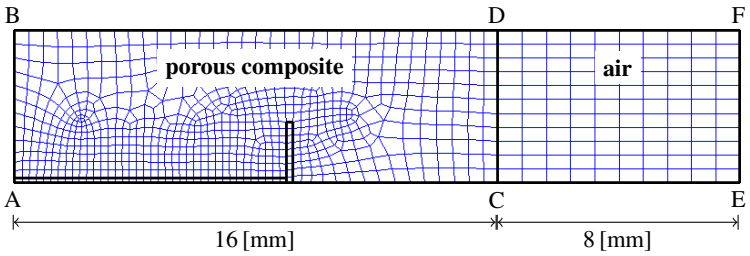

Figure A1: Finite-element mesh of the model with an adjacent layer of air.

To prove the validity of the averaging approach, Figure A2 compares some absorption curves for the foam-B composite with T-shaped inclusions, computed using the model shown in Figure 2, with the curve computed using the extended model of the porous composite with an adjacent domain of air (see Figure A1), 8 mm-thick, which is sufficient for the wave to be plane at the boundary of the domain (i.e., along the line EF in Figure A1). It is clearly visible that the averaging result – curve (c) in Figure A2 – and the result calculated from the extended model with layer of air – curve (d) in Figure A2 – are almost identical; some very small discrepancies appear only in a higher frequency range – above 3 kHz – and this is correlated with the observation that in that very range the curves taken to calculate the arithmetic average are rather different from each other, yet they differ from the correct result in a sort of symmetrical way. It was checked that the same conclusions can be drawn in case of foam A and other configurations.

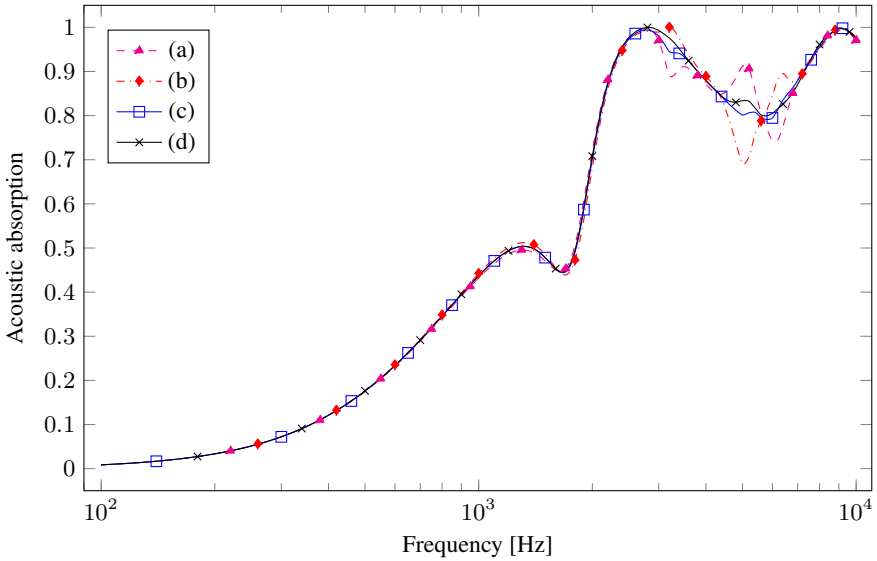

Figure A2: Passive absorption curves for the foam-B composite with T-shaped inclusions: (a) the absorption computed at point C of the economical model ABCD, (b) the absorption computed at point D of the economical model ABCD, (c) the averaged curve obtained from these two curves, (d) the absorption curve computed anywhere on the line EF of the extended model ABCDEF with the adjacent 8 mm-thick layer of air.

References

[1] M. R. F. Kidner, C. R. Fuller, B. Gardner, Increase in transmission loss of single panels by addition of mass inclusions to a poro-elastic layer: Experimental investigation, J. Sound Vib. 294 (2006) 466–472.

[2] F.-C. Lee, W.-H. Chen, On the acoustic absorption of multi-layer absorbers with different inner structures, J. Sound Vib. 259 (4) (2003) 761–777.

[3] N. Dauchez, S. Sahraoui, N. Atalla, Investigation and modelling of damping in a plate with a bonded porous layer, J. Sound Vib. 265 (2003) 437–449.

[4] T. Yamamoto, S. Maruyama, S. Nishiwaki, M. Yoshimura, Topology design of multi-material soundproof structures including poroelastic media to minimize sound pressure levels, Comput. Methods Appl. Mech. Engrg. 198 (2009) 1439–1455.

[5] C. A. Gentry, C. Guigou, C. R. Fuller, Smart foam for applications in passive-active noise radiation control, J. Acoust. Soc. Am. 101 (4) (1997) 1771–1778.

[6] C. Guigou, C. R. Fuller, Adaptive feedforward and feedback methods for active/passive sound radiation control using smart foam, J. Acoust. Soc. Am. 104 (1) (1998) 226–231.

[7] C. Guigou, C. R. Fuller, Control of aircraft interior broadband noise with foam-PVDF smart skin, J. Sound Vib. 220 (3) (1999) 541–557.

[8] J. Tang, T. Wang, Piezocomposite smart foam for active control of underwater noise, in: Proceedings of Global Congress on Intelligent Systems, 2009.

[9] J.-K. Lee, J. Kim, C.-J. Rhee, C.-H. Jo, S.-B. Choi, Noise reduction of passive and active hybrid panels, Smart Mater. Struct. 11 (2002) 940–946.

[10] N. Sellen, M. Cuesta, M.-A. Galland, Noise reduction in a flow duct: Implementation of a hybrid passive/active solution, J. Sound Vib. 297 (2006) 492–511.

[11] J. F. Allard, Propagation of Sound in Porous Media. Modelling Sound Absorbing Materials, Elsevier, 1993.

[12] J. F. Allard, N. Atalla, Propagation of Sound in Porous Media: Modelling Sound Absorbing Materials, Second Edition, Wiley, 2009.

[13] M.-A. Galland, J.-B. Dupont, A new hybrid passive/active cell to realize a complex impedance boundary condition, in: Conference Proceedings of Acoustics'08, 2008.

[14] J.-B. Dupont, M.-A. Galland, Active absorption to reduce the noise transmitted out of an enclosure, Appl. Acoust. 70 (2009) 142–152.

[15] T. G. Zielinski, M.-A. Galland, M. N. Ichchou, Active reduction of vibroacoustic transmission using elasto-poroelastic sandwich panels and piezoelectric materials, in: Proceedings of SAPEM'2005: Symposium on the Acoustics of Poro-Elastic Materials, Lyon, France, 2005.

[16] T. G. Zielinski, M.-A. Galland, M. N. Ichchou, Further modeling and new results of active noise reduction using elasto-poroelastic panels, in: Proceedings of ISMA2006: International Conference on Sound and Vibration, Leuven, Belgium, Vol. 1-8, 2006, pp. 309–319.

[17] C. Batifol, T. G. Zielinski, M. N. Ichchou, M.-A. Galland, A finite-element study of a piezoelectric/poroelastic sound package concept, Smart Mater. Struct. 16 (2007) 168–177.

[18] C. Batifol, M. Ichchou, M.-A. Galland, Component mode synthesis finite element model of a smart double-plate panel, in: Conference Proceedings of 19th International Congress on Acoustics ICA2007, 2007.

[19] P. Leroy, A. Berry, N. Atalla, P. Herzog, Numerical analysis of smart foam for acoustic absorption, in: Conference Proceedings of 19th International Congress on Acoustics ICA2007, 2007.

[20] P. Leroy, P. Herzog, A. Berry, N. Atalla, Experimental assessment of the performance of a smart foam absorber, in: Conference Proceedings of Acoustics'08, 2008.

[21] P. Leroy, N. Atalla, A. Berry, P. Herzog, Three dimensional finite element modeling of smart foam, J. Acoust. Soc. Am. 126 (6) (2009) 2873–2885.

[22] F. Scarpa, F. C. Smith, Passive and MR fluid-coated auxetic PU foam – mechanical, acoustic, and electromagnetic properties, J. Intell. Mater. Syst. Struct. 15 (2004) 973–979.

[23] F. Scarpa, W. A. Bullough, P. Lumley, Trends in acoustic properties of iron particle seeded auxetic polyurethane foam, Proc. Inst. Mech. Eng. Part C J. Mech. Eng. Sci. 218 (2) (2004) 241–244.

[24] T. G. Zielinski, M. Rak, Acoustic absorption of foams coated with MR fluid under the influence of magnetic field, J. Intell. Mater. Syst. Struct. 21 (2010) 125–131.

[25] T. G. Zielinski, Active porous composites for wide frequency-range noise absorption, in: Proceedings of ISMA2008: International Conference on Sound and Vibration, Leuven, Belgium, Vol. 1-8, 2008, pp. 89–103.

[26] T. G. Zielinski, Fundamentals of multiphysics modelling of piezo-poro-elastic structures, Archives of Mechanics 62 (5) (2010) 343–378.

[27] T. G. Zielinski, Multiphysics modeling and experimental validation of the active reduction of structure-borne noise, Journal of Vibration and Acoustics – Transactions of the ASME 132 (6) (2010) 061008–1–14.

[28] N. Atalla, M. A. Hamdi, R. Panneton, Enhanced weak integral formulation for the mixed (u,p) poroelastic equations, J. Acoust. Soc. Am. 109 (6) (2001) 3065–3068.

[29] P. Debergue, R. Panneton, N. Atalla, Boundary conditions for the weak formulation of the mixed (u,p) poroelasticity problem, J. Acoust. Soc. Am. 106 (5) (1999) 2383–2390.

[30] A. Benjeddou, Advances in piezoelectric finite element modeling of adaptive structural elements: a survey, Comput. Struct. 76 (2000) 347–363.

[31] I. Harari, A survey of finite element methods for time-harmonic acoustics, Comput. Methods Appl. Mech. Engrg. 195 (2006) 1594–1607.

[32] L. L. Thompson, A review of finite-element methods for time-harmonic acoustics, J. Acoust. Soc. Am. 119 (3) (2006) 1315–1330.

[33] D. Givoli, High-order local non-reflecting boundary conditions: a review, Wave Motion 39 (2004) 319–326.

[34] S. Rigobert, F. C. Sgard, N. Atalla, A two-field hybrid formulation for multilayers involving poroelastic, acoustic, and elastic materials, J. Acoust. Soc. Am. 115 (6) (2004) 2786–2797.

[35] M. A. Biot, The theory of propagation of elastic waves in a fluid-saturated porous solid, J. Acoust. Soc. Am. 28 (2) (1956) 168–191.

[36] N. Dauchez, S. Sahraoui, N. Atalla, Convergence of poroelastic finite elements based on Biot displacement formulation, J. Acoust. Soc. Am. 109 (1) (2001) 33–40.

[37] N. Atalla, R. Panneton, P. Debergue, A mixed displacement-pressure formulation for poroelastic materials, J. Acoust. Soc. Am. 104 (3) (1998) 1444–1452.

[38] D. Givoli, B. Neta, High-order non-reflecting boundary scheme for time-dependent waves, J. Comput. Phys. 186 (2003) 24–46.

[39] J. F. Allard, C. Depollier, P. Guignouarad, P. Rebillard, Effects of a resonance of the frame on the surface impedance of glass wool of high density and stiffness, J. Acoust. Soc. Am. 89 (3) (1991) 999–1001.

[40] O. Doutres, N. Dauchez, J.-M. Génevaux, O. Dazel, Validity of the limp model for porous materials: A criterion based on the Biot theory, J. Acoust. Soc. Am. 122 (4) (2007) 2038–2048.

[41] F. C. Sgard, N. Atalla, J. Nicolas, A numerical model for the low frequency diffuse field sound transmission loss of double-wall sound barriers with elastic porous linings, J. Acoust. Soc. Am. 108 (6) (2000) 2865–2872.

[42] O. Dazel, F. Sgard, F.-X. Becot, N. Atalla, Expressions of dissipated powers and stored energies in poroelastic media modeled by $\{\mathbf{u}\text{-}\mathbf{U}\}$ and $\{\mathbf{u}\text{-}P\}$ formulations, J. Acoust. Soc. Am. 123 (4) (2008) 2054–2063.